Experimental study of chemical conversion of methanol and ethylene glycol in a film boiling reactor

Sung Ryel Choi, John W. Evangelista [1], C. Thomas Avedisian *, Wing Tsang [2]

Sibley School of Mechanical and Aerospace Engineering, Cornell University, Ithaca, NY 14853-7501, USA

ABSTRACT

Film boiling on a horizontal tube is used to convert methanol and ethylene glycol to synthesis gas and other species by thermal decomposition and catalytic reaction. Methanol reacts on a platinum catalyst to form CO and H_2 in near stoichiometric proportions while ethylene glycol products include additional condensable and soluble species. The influence of catalyst degradation on prolonged operation is suggested as a cause for some of the trends observed. Product yields for thermal decomposition of methanol are quite repeatable while for ethylene glycol significant carbon deposits appear to produce greater variability in the measured product flow rates.

© 2010 Elsevier Ltd. All rights reserved.

1. Introduction

The idea of exploiting the high surface temperatures associated with film boiling to promote chemical change of a liquid arises from thermal runaway scenarios that can occur in the liquid/liquid interactions associated with nuclear reactor safety. The interaction of water with molten metals (such as zirconium or lithium) is an example. When subcooled water comes into intimate contact with a molten metal that is hundreds of degrees hotter, the water can flash evaporate and insulate the molten material from the bulk by a vapor layer. The steam within the layer can react with the metal to form metal oxides and hydrogen [1–7]. Later studies illustrated the capability of film boiling to convert organic liquids on bare heated surfaces, and to form solid deposites on them [8–12]. Indirect evidence of reaction has included measurement of a gas flow associated with a heated horizontal wire in a stagnant pool of an organic liquid [13] and enhancement of the heat transfer coefficient in film boiling on a tube coated with catalyst [14]. Theoretical modeling of film boiling with chemical reaction has considered the horizontal tube and vertical plate configurations. Film boiling was analyzed for water on a vertical zirconium plate to study the hydrogen produc-

tion process [15]. The horizontal tube geometry, which is especially suited to model film boiling and the companion problem of film condensation [16], was used to analyze the effects of radiation and surface temperature and to model catalytic reaction with certain simplifying assumptions [14,17,18].

The present study reports an experimental effort to measure the efficacy of film boiling to convert organic liquids by both thermal decomposition and catalytic means. A horizontal tube is positioned in a stagnant pool of a reactant organic liquid, the tube temperature is raised to where film boiling is initiated, and the product gas stream is monitored and chemically analyzed to infer reaction pathways. The working fluids are methanol (CH_3OH, boiling point of 338 K) and ethylene glycol ($C_2H_4(OH)_2$, boiling point of 467 K) because of their industrial relevance (e.g., ethylene glycol is used as an antifreeze agent in cooling and heating systems, in hydraulic brake systems and electrolytic condensers, in some paints, plastics, inks, wood stains, and adhesives, and as an aircraft de-icer; methanol is used in the trans-esterification process of biodiesel production, in direct methanol fuel cells to produce electricity, as an extraction agent in the oil and food industries, and in wastewater treatment processes to convert nitrates to nitrogen). Methanol and ethylene glycol also represent "light" and "heavy" molecules, respectively, which will allow assessing the versatility for conversion by film boiling, and their decomposition chemistry is reasonably known.

Fig. 1 is a schematic of the film boiling structure on a horizontal tube that illustrates the transport paths involved. Reactant vapors enter the vapor film by evaporating at the liquid/vapor interface,

* Corresponding author. Tel.: +1 607 592 7915; fax: +1 607 255 1222.
  E-mail address: cta2@cornell.edu (C.T. Avedisian).
[1] Present address: Department of Mechanical Engineering, United States Military Academy, West Point, NY, 10996, USA.
[2] Present address: Physical and Chemical Properties Division, National Institute of Standards and Technology, Gaithersburg, MD 20899, USA.

Nomenclature

A_o	outer surface area of a tube (m²)		X	conversion (Eq. (1))
d_i	tube inner diameter			
d_o	tube outer diameter		*Greek letters*	
C_p	specific heat (J mol⁻¹ K⁻¹)		α_i	stoichiometric coefficient of species i
$\bar{h}$	enthalpy per unit of mole (J mol⁻¹)		δ	vapor film thickness (m)
$\bar{h}$	convective heat transfer coefficient (W m⁻² K⁻¹)		v	summation of stoichiometric coefficients of product gas
ΔH_{fg}	heat of vaporization (J mol⁻¹)			
ΔH_{rxn}	heat of reaction (J mol⁻¹)		*Subscripts*	
k	thermal conductivity (W m⁻¹ K⁻¹)		in/out	control volume inlet/outlet
$\dot{N}$	molar flow rate (mol sec⁻¹)		P	product
T	temperature (K)		R	reactant
T_{wall}	tube wall temperature (K)		sat	saturation condition
ΔT_{sub}	subcooling $(= (T_{sat} - T_\infty))$ (K)		∞	bulk liquid

and vapor flow around the tube within the film is driven by buoyancy (forcing the flow of the liquid around the tube could enhance the effect, but in this study we consider the pool boiling case). As the vapor flows around the tube reactions can occur at rates appropriate to the gas temperature. The reactions are confined to a layer that is bounded on one side by the tube surface and on the other by the distance from the wall where the temperature remains above the threshold value for reactions to occur at appreciable rates. This layer is comparatively thin as the wall temperature is on the order of a thousand degrees while the temperature of the liquid/vapor interface is close to the liquid boiling point. Products are transported by bubbles that pinch off and percolate through the bulk liquid pool as is typical of film boiling. This process of evaporation, vapor transport and chemical reaction within the vapor film defines what is termed a film boiling reactor or "FIBOR" [17]. Though the idea of promoting chemical reaction by film boiling does not have the flexibility of conventional systems (e.g., standard plug flow or static reactors), its chief advantage is its simplicity, that a FIBOR will be self-assembled, and that it is scalable. Because the boiling curve and the structure of the vapor film are so important to delineating the operational domain of a FIBOR, boiling curves for

methanol and ethylene glycol are also reported for bare tubes and tubes coated with a catalyst.

The conversion chemistries for methanol and ethylene glycol are mainly endothermic, with carbon monoxide (CO) and hydrogen (H_2) as the principle products. For methanol, the primary unimolecular reaction is speculated to be:

$$CH_3OH \rightarrow CO + 2H_2, \tag{1}$$

with a heat of reaction (ΔH_{rxn}°) of 91 kJ/mol, while for ethylene glycol it is

$$C_2H_4(OH)_2 \rightarrow 2CO + 3H_2, \tag{2}$$

with $\Delta H_{rxn}^\circ = 173$ kJ/mol [19]. Eqs. (1) and (2) frame the conversion of methanol and ethylene glycol in simple terms, as the intent here is not to present details of kinetic mechanisms in a FIBOR but rather to show its potential for affecting chemical change of a liquid at bulk subcooled temperatures.

Secondary reactions may be indicated by formation of additional species in the product gas stream such as methane (CH_4) [20]:

$$CO + 3H_2 \rightarrow CH_4 + H_2O, \tag{3}$$
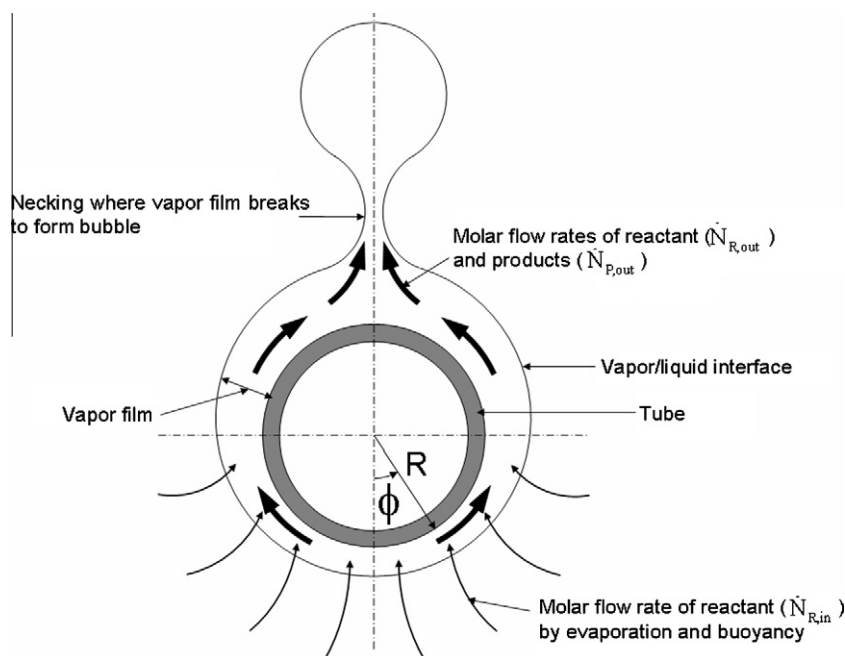
Fig. 1. Idealized schematic o film boiling around a horizontal tube or radius R showing liquid and vapor flow paths (arrows). Not to scale.

carbon or coke [9,21] through reaction with methane:

$$CH_4 \rightarrow 2H_2 + C, \tag{4}$$

or from decomposition of carbon monoxide:

$$2CO \rightarrow O_2 + 2C, \tag{5}$$

as well as from the decomposition of other hydrocarbons such as acetylene (C_2H_2). Additional reaction pathways would also be suggested if the bulk liquid pool became contaminated with condensable species during prolonged operation of the FIBOR. This aspect is further discussed in Section 3.2.2.

2. Experiments

2.1. Apparatus

A schematic of the experimental apparatus is shown in Fig. 2(a). It provides for development of film boiling on a horizontal tube, control of power to the tube, monitoring the relevant temperatures and chemical analysis of the products. The operational parameters include tube input power, tube wall temperature (T_w), and bulk

liquid subcooling. In this section, we outline the design of a FIBOR and procedures for creating it. Further details are given in [22,23].

The apparatus consists of three modules: the "FIBOR module" which includes a glass chamber (3 L volume) that contains the reactant liquid and the tube around which the FIBOR is created; a "condenser module" comprised of condensers and vapor traps that condense and remove reactant vapors from the out-gas stream; and a "data acquisition and chemical detection module" that includes the data acquisition and control system assembly which consists of a programmable DC power supply (Agilent #6681A) for heating the tube, digital flow meter (Omega #FMA-A2309) for measuring product gas flow rates, and a mini-pump arrangement (Fig. 2(b)) for product gas injection directly into a gas chromatograph (GC, GOW-MAC Instrument Series 600-TCD). The GC targeted detection of N_2, CO, H_2, CH_4, C_2H_2 and C_2H_4. Before the output gas is exhausted, a small volumetric flow ($\sim$30 ccm) is withdrawn and introduced directly into the GC by the mini-pump arrangement shown in Fig. 2(b). The GC analyzes product gases at steady state during an experiment. In addition to gas phase analysis, liquid composition was assessed by GC/MS analysis using an Agilent Technologies 6890 N/5973 system. The experiment is controlled by LabVIEW which adjusts input voltage and current
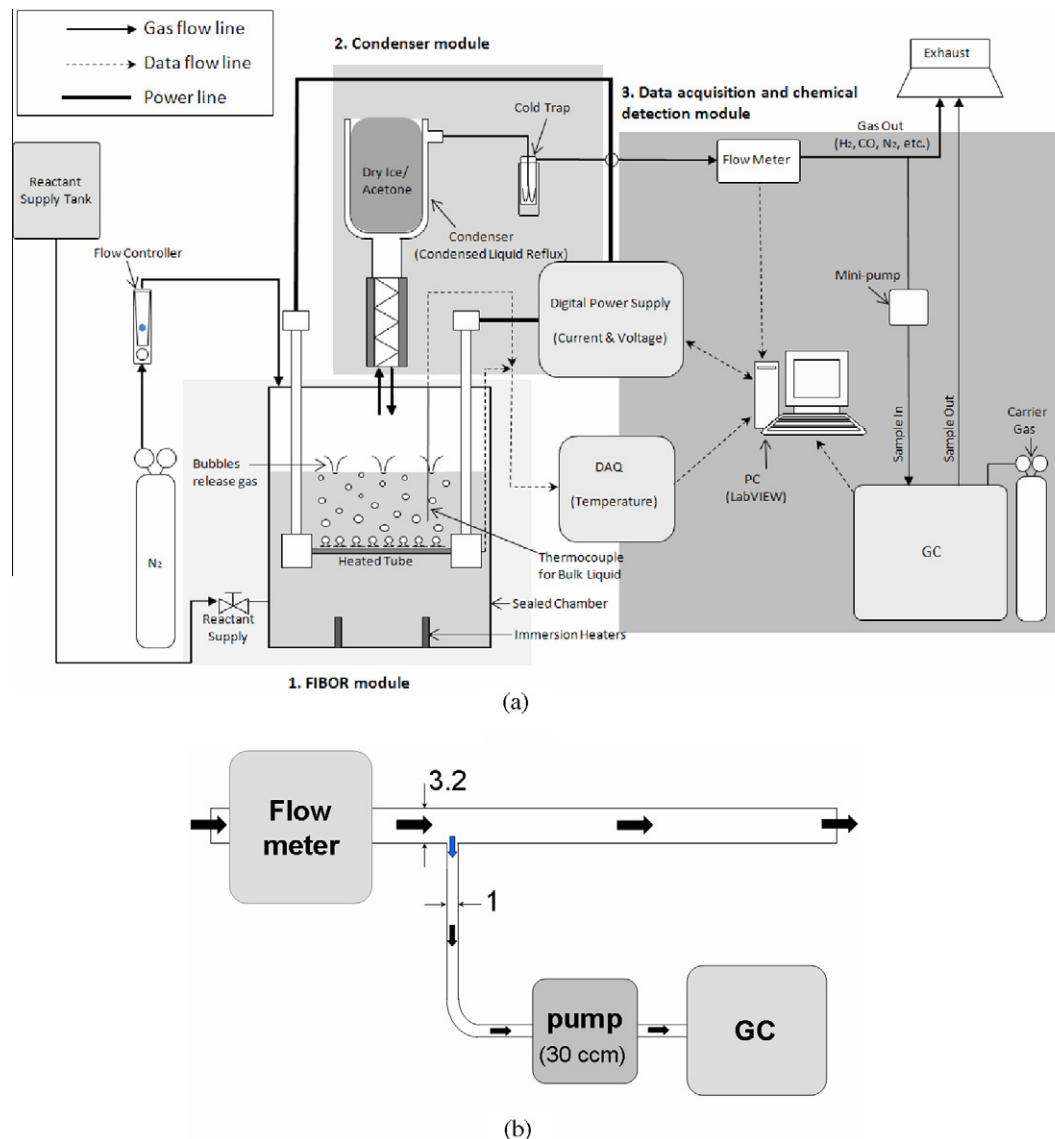
Fig. 2. (a) Schematic of experimental apparatus; (b) gas sampling system for GC (numbers denote millimeters).

supplied to the heater, records the volumetric flow rate of product gases, the power to the tube (voltage and current) and thermocouple outputs.

Considering the two main methods of establishing film boiling – by controlling tube power or tube temperature – we employed a power-controlled process because of the relative ease of operation. Certain portions of the boiling curve are inaccessible when input power is the control variable (i.e., the transition boiling regime) but this limitation does not overly restrict the operational domain of the FIBOR nor hinder demonstration of the concept.

Tubes for supporting FIBORs were fabricated from a nickel alloy (Inconel 600, melting point of 1686 K). Fig. 3(a) is a schematic of the tube assembly showing location of thermocouples for temperature measurement. The tubes are 4.76 mm O.D., 3.34 mm I.D., and 140 mm long. Electrical power is delivered to the tube by 13 mm diameter copper rod busses attached to clamps at each end of the tube. The busses are passed through the top flange of the glass chamber by electrical feed-throughs and then connected to the power supply by clamps. Thermocouples (i.e., Omega #KMQXL-010G-18 thermocouples) are used to measure tube temperature at the locations shown in Fig. 3(a). The temperature was found to be reasonably uniform over the central 60 mm of the tube, as shown by representative measurements in Fig. 3(b) for film boiling in methanol. The decrease at the ends is due to heat losses through the copper clamps which created some issues with film boiling stabilization over prolonged periods as discussed in Section 3.2.

At the higher temperatures imposed on the tubes (~1300 K), they tended to sag somewhat due to structural considerations. To counteract this tendency the tubes were fitted with a single-hole ceramic rod insert (Omega #ORX-11618 ceramic tube) through which the thermocouples were inserted. This insert also provided electrical isolation of the thermocouples from the tube wall. The tube ends were sealed with Dow Corning 736 Heat Resistant Sealant. Catalyst coatings covered the central 92 mm of the tube.

2.2. Procedure

For tubes coated with a catalyst, the procedure for establishing film boiling must minimize or avoid entirely liquid contact so that the catalyst is not deactivated. This matter is not a concern for a bare tube. Fig. 4 schematically illustrates our procedure for establishing film boiling. The tube is first pre-heated to about 600 K in an empty chamber in the presence of a 50 ccm flow of nitrogen as a precaution against igniting the organic vapors that are produced by heat transfer from the hot tube to the cold liquid. The bulk pool reactant temperature is increased to the desired value by four immersion heaters installed in the chamber and the liquid level is then raised by drawing liquid into the chamber to about 15 mm below the heater (Fig. 4(a)). During this period, vapors are produced by the proximity of the hot tube to the liquid surface and the activity of the catalyst can be assessed by monitoring both the flow meter and GC output. If the catalyst is active, a chemical reaction will be detected by a non-zero flow through the meter in the "data acquisition and chemical detection" module (Fig. 2(a)) and the immersion process is then continued. If the catalyst is not active, the process is terminated (though continued for
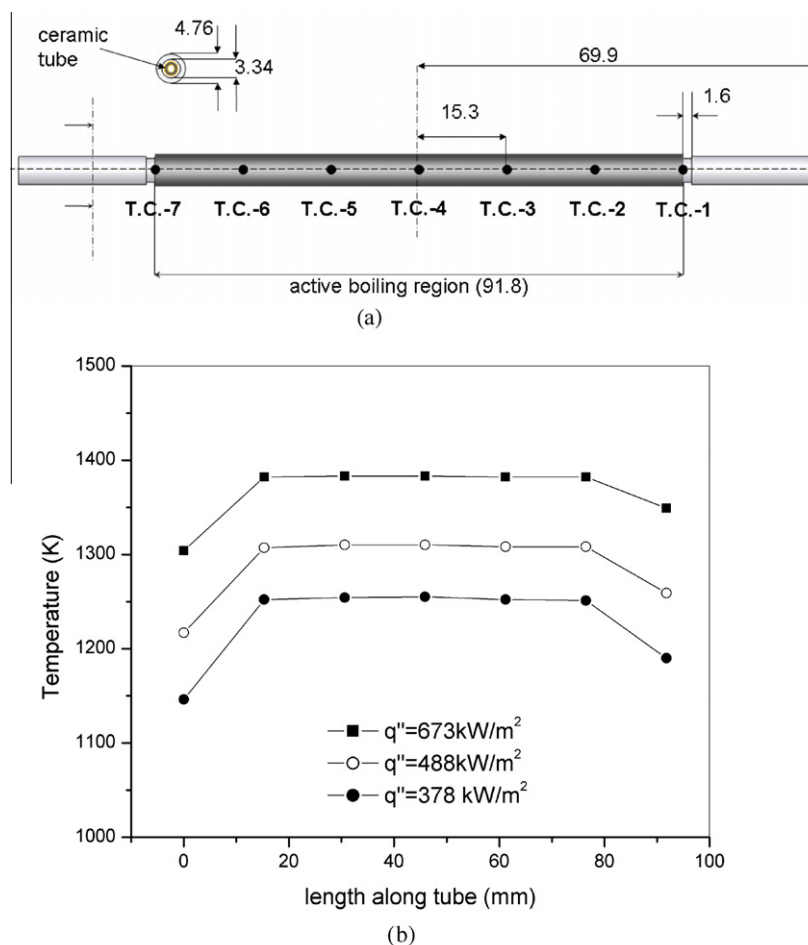
Fig. 3. (a) Detail of heater tube assembly showing thermocouple positions (numbers denote millimeters); (b) variation of surface temperature with position along a tube for three heat flux settings in methanol.
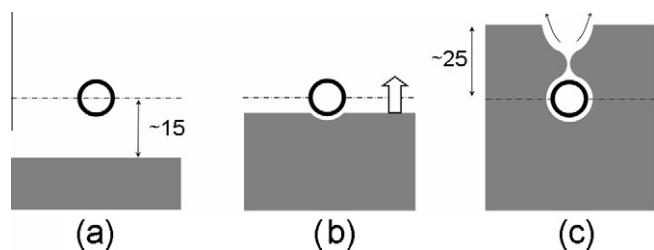
Fig. 4. Procedure for creating film boiling. Gray area is liquid; tube is black ring; numbers denote millimeters. At "a", reactability of catalyst can be assessed before proceeding to "b" and "c".

a bare tube). The temperature of the tube surface is then further increased to about 800 K.

Raising the liquid level around the tube, now at about 800 K, is coordinated with adjusting power to the tube to avoid film destabilization (Fig. 4(b)). The process is similar to that described by Ede and Siviour [24]. As the liquid level appears to just touch the bottom of the tube and a quenching effect noted, power is increased by a factor of 4 through manual adjustment in order to maintain the wall temperature at 800 K to reach the condition of Fig. 4(c). Once in film boiling, the liquid level is kept approximately 25 mm above the tube. Though it was not necessary to use this immersion process for bare tubes, the alternative of progressing through the range of powers (nucleate boiling, critical heat flux (CHF), film boiling) after initially submerging a bare tube was also somewhat problematic by virtue of the tendency for a rapid wall temperature excursion to occur at the CHF point, and the potential for physically damaging the tube by overheating it. As such, the catalyst procedure was also used for bare tubes.

2.3. Catalyst preparation

Three tube surface preparations are reported as summarized in Table 1: CT#1 for methanol which consisted of an alumina oxide (Al_2O_3) layer impregnated with 55% by weight platinum black (Pt); CT#2 for ethylene glycol with 38% by weight Pt; and bare tubes. Since the primary intent was to examine the extent to which film boiling could promote chemical change and to accurately measure the product gases formed and associated product yields (flow rates) no attempt was made here to systematically vary catalyst parameters.

Catalysts were applied by Catacel Corp (Garrettsville, OH) using a three-step process: (1) oxidation of the tube surface; (2) creation of an aluminum oxide adhesion layer; and (3) application of the platinum catalyst by impregnation of an alumina layer. In the first step, a clean bare tube is roughened (with #320 grit paper) and then baked in an oven at 900 °C for 4 h. In the second step, a "washcoat" is applied to the tube using a pipette to drip it over the tube which is rotating at about 30 rpm (the washcoat is an aqueous gamma alumina solution with pH 3). The washcoated tube is then baked at 800 °C for 5 h. The second step is repeated at least five times until a uniform alumina layer is deposited. In the third step, a tetra amine platinum nitrate solution with pH 3 is applied by dripping from a pipette while the tube is rotating. The tube is then baked in an oven at 500 °C for 1 h in a flowing mixture of 96% argon and 4% hydrogen for reduction.

Fig. 5 is an SEM of the catalyst structure for CT#1 before (a) and after (b) creating a FIBOR in methanol through two cycles (i.e., creating a FIBOR, cool-down, then repeating). The black regions in Fig. 5(b) are carbon deposits that suggest one or more of the carbon formation reactions discussed in Section 1. For all results presented here, the wall temperatures for the catalyst-coated tubes were kept below about 1300 K. At higher temperatures significant structural changes of the coatings were noted, and the tubes themselves appeared to bend (hence the reason for the ceramic insert). Bare tubes were heated to higher values (to about 1500 K).

3. Results

3.1. Boiling curves

Fig. 6(a) and (b) show boiling curves for bare tubes, CT#1 and CT#2 at the indicated bulk liquid subcoolings. The nucleate boiling portion of the boiling curve is shown only for the bare tubes since, as noted previously, the catalyst would deactivate by liquid contact so that nucleate boiling was not imposed for the catalyst tubes. For both fluids, the upper flux in the nucleate boiling portion of the curve for the bare tubes was close to the critical heat flux above which one or more hot spots developed that created the danger of melting. The measured CHF values are considerably lower than reported by Fugita and Bai [25], which is likely the result of their having used small diameter wires (0.5 mm) as compared to almost 5 mm here where the heater diameter influences CHF [25,26]. The data to the right of nucleate boiling portion correspond to film boiling. The FIBOR operates in this domain.

As temperature is increased for the bare tubes in Fig. 6(a) and (b) the heat flux dissipated increases accordingly but it is not possible to determine conclusively from these data if a reaction occurs. The elevated heat flux for the catalyst tubes could be due either to reaction (since the primary reactions of Eqs. (1) and (2) are endothermic) or an enhancement of the surface area of the catalyst coating that promotes an increase of active boiling sites. The difference in heat input between the catalyst and bare tube data for methanol is quite close to the heat of reaction for the primary decomposition reaction (Eq. (1)) thus suggesting that the higher fluxes for the catalyst tubes do evidence reaction.

The boiling curve for ethylene glycol (Fig. 6(b)) exhibits similar features to methanol, but the interpretation is more complicated for several reasons. Firstly, the difference between the bare and catalyst tube fluxes is not entirely the heat of reaction for Eq. (2), which indicates that the conversion chemistry for ethylene glycol is more complicated than methanol. Secondly, below about $T_w \approx 1150$ K there is a noticeable change in heat flux or wall temperature which is caused by destabilization or collapse of film boiling as confirmed by visual observations of nucleate boiling near the ends of the tube where it was clamped to the electrodes. With destabilization over a portion of the tube surface, the power dissipated, averaged over the entire tube length (which is what we measure), should increase for a given temperature because of the effect of nucleate boiling. As a final note, the addition of a coating such as from a catalyst adds a thermal resistance to the tube that should lower the flux for a given temperature or increase the temperature for a given flux if the coating is passive and only adds a

Table 1
Tube surface conditions.

	Alumina (g)	Pt (g)	Wt.% of Pt	Total wt. (g) (before/after)	Thickness of alumina (mm)
CT#1, Methanol	0.045	0.054	55	0.099/0.118	0.008
CT#2, Ethylene glycol	0.047	0.029	38	0.076/0.087	0.009
Bare tube	–	–	–	–	–
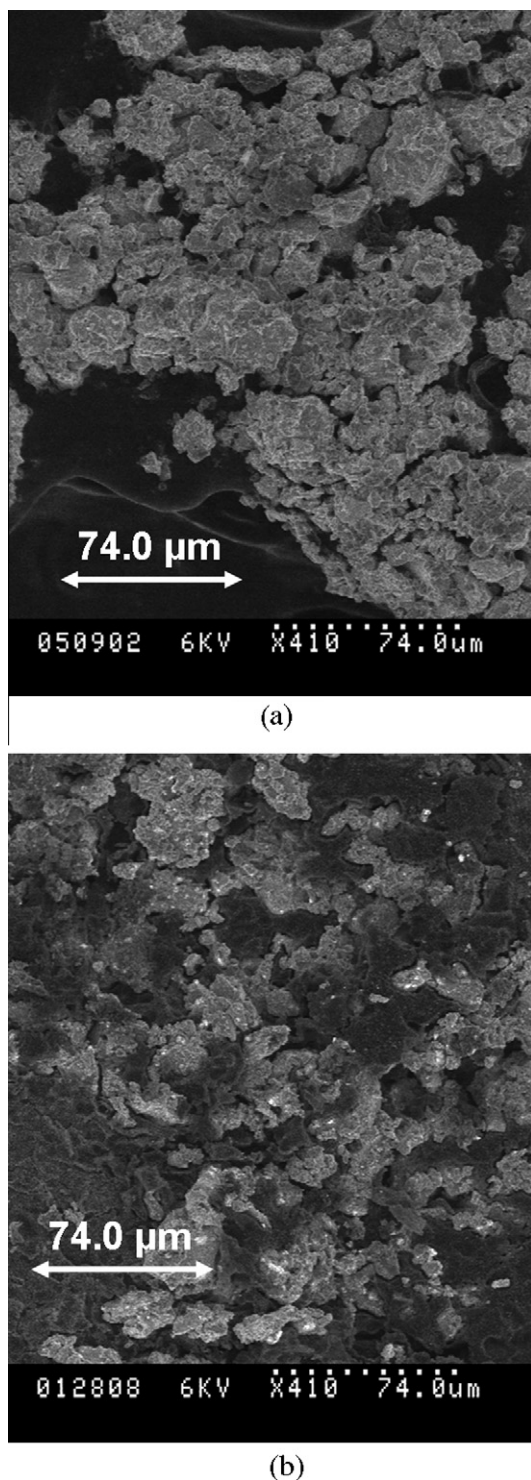
Fig. 5. SEM pictures of catalyst structure (CT#1; see Table 1) before (a) and after (b) creating a FIBOR.

Fig. 6. Boiling curve for (a) methanol and (b) ethylene glycol at the indicated subcoolings. Solid circles show fluxes for a FIBOR on a catalyst. Open circles are for bare tube. Lower limit on film boiling fluxes is determined by film destabilization.

purely conductive resistance to the tube. Fig. 6(a) and (b) show that neither of these trends is found.

3.2. Product yields

3.2.1. Methanol

Two means were used to determine if a reaction occurred: measuring a non-zero product gas flow rate; and out-gas GC analysis.

As noted previously, the system of condensers and vapor traps was designed to remove reactant vapor from the out-gas stream for methanol. As such, any non-zero flow would then only be from noncondensable gases formed by reaction.

Fig. 7 shows the variation of out-gas flow rate with wall temperature for CT#1 at 14 K subcooling. The numbers correspond to the sequence of power adjustments that were executed. Starting with the tube positioned as in Fig. 4(a) ("1" in Fig. 7), the first evidence of reaction was observed at about 600 K where methanol vapors surrounded the tube as it was evaporated by the proximity of the tube to the liquid surface. Continuing to increase the temperature, at 850 K (2) the process of raising the liquid level and coordinating power to the tube to counteract the effects of quenching began (Fig. 4(b)). Upon full immersion with a coordinated power increase to "3", film boiling was established (Fig. 4(c)) and the product yield increased from 2500 L/m/m^2 to almost 8000 L/min/m^2. After (3) the power was varied along the film boiling portion of the boiling curve: from 3 to 4 then back down to 5, up to 6, down to 7 and up to 8. At several of these temperature excursions, the out-gas was directed to the GC for chemical analysis. From this analysis, the molar ratio of CO to H$_2$ was determined by analyzing the GC trace.

Fig. 8 shows greater detail of the product yields in Fig. 7. Two developments of the FIBOR are shown. The data were obtained after the initial FIBOR (open circles) was destroyed by turning off power to the tube and the liquid allowed to cool to room temperature. The lower bound on the data at 920 K corresponds
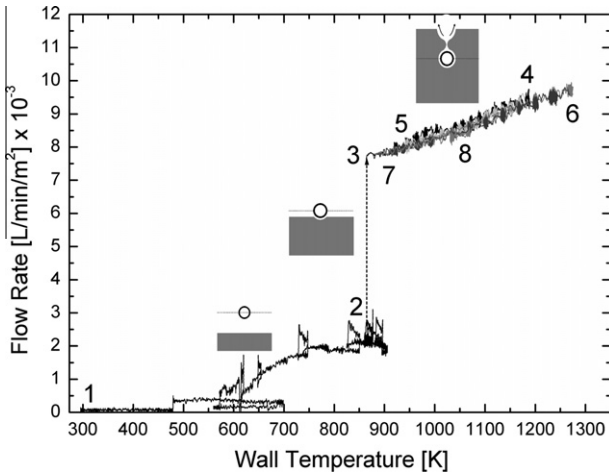
Fig. 7. Variation of flow rate of product gas with wall temperature for CT#1 in methanol. Numbers correspond to stages of power input. Reactability at "2" is assessed with tube positioned above liquid pool before immersion.
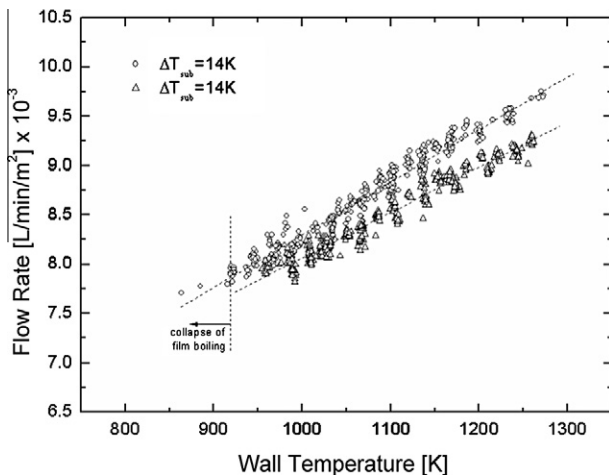
Fig. 8. Variation of product flow rates with T_w for methanol on CT#1 for two different developments of a FIBOR at 14 K subcooling. Open triangle data were obtained after FIBOR was turned off, the methanol pool was allowed to cool to room temperature, and the FIBOR reconstituted. The lower temperature limit of FIBOR is determined by destabilization of the vapor film.

to destabilization of the vapor film (recalling that two conditions must be met for the FIBOR: the film must be supported and the temperature must be high enough to drive the reaction). There is a noticeable reduction of product yield after the second realization of the FIBOR. This reduction is most likely due to the fact that the catalyst had materially changed after the first FIBOR through a variety of mechanisms: carbon deposits from coke formation reactions (Eqs. (3)–(5) and Fig. 5) infiltrating the catalyst; sintering of pores as a result of exposure to high operating temperatures particularly in the presence of hydrogen in which the pores could tend to fuse [27,28]; or catalyst de-lamination or detachment caused by changes in surface temperature during the quenching procedure or during the normal course of exposure to high temperatures and the cool-down period associated with termination of an experiment.

For thermal decomposition (film boiling on a bare tube), none of the variations shown on CT#1 were observed. Fig. 9 shows the product gas flow rate for methanol. The two sets of data in Fig. 9 were taken after the initial FIBOR was destroyed by turning off power, allowing the tube and surrounding methanol to cool to room temperature, cleaning the tube surface, and reconstituting
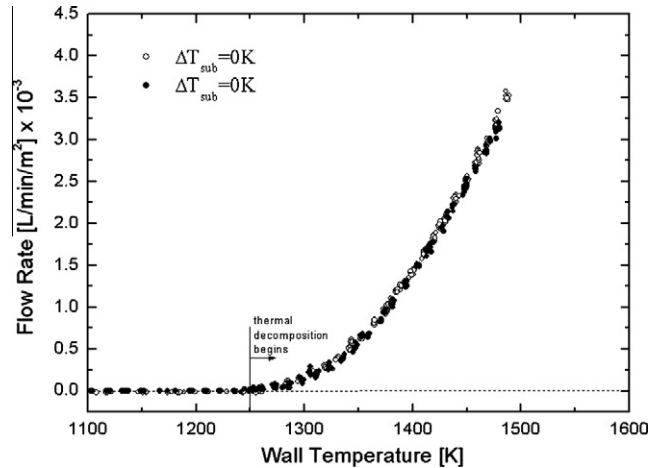
Fig. 9. Variation of product flow rates with T_w on a bare tube in saturated methanol. There is no detectable evidence of reaction below about 1250 K.

the FIBOR. The repeatability between the two realizations of the FIBOR is now excellent, and is believed to be due to the comparatively unchanging character of the bare surface during film boiling. Below about 1250 K, the conversion is essentially zero indicating no reactability of methanol on a bare tube. Above 1250 K the product gas flow rate increases, at first in a somewhat exponential-like manner then it becomes linear with tube temperature. Comparing Figs. 8 and 9, the products formed on CT#1 for methanol are due only to a catalytic effect, as without a catalyst (Fig. 9) the tube temperature is too low to thermally decompose methanol at the temperatures of Fig. 8.

The identification and analysis of the species in the product gases was determined by GC analysis of the gas stream. Fig. 10 shows the results for CT#1 where the variation of molar ratio of CO to H_2 with temperature is shown. The inset is a representative GC trace, here being at 1018 K where the primary chemical species detected are H_2, CH_4, N_2 and CO. As noted previously, N_2 in the GC trace is the result of introducing it into the gas above the methanol pool during the immersion process of Fig. 4 as a safety precaution to prevent the possibility of ignition (the N_2 flow was turned off for ethylene glycol after creating the FIBOR as experienced was gained). The presence of small amounts of CH_4 indicates the
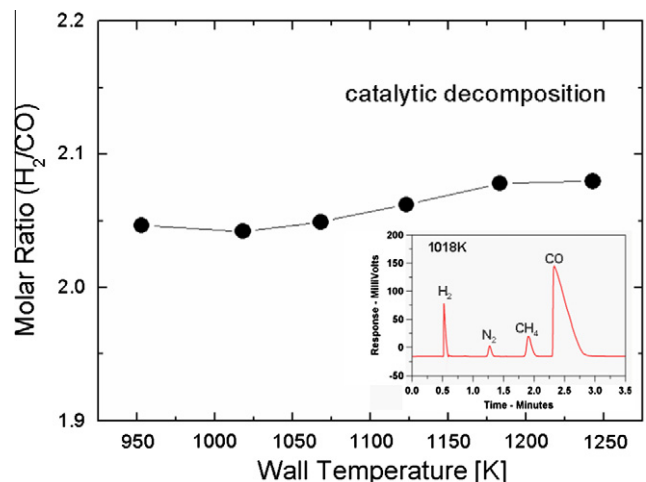
Fig. 10. Variation of molar ratio of H_2 to CO with wall temperature for methanol on CT#1 based on GC traces obtained while tube was at the indicated wall temperature (the inset shows a GC trace obtained while T_w was 1018 K). N_2 is from a trickle flow to prevent ignition of methanol vapors.

potential of Eq. (3) and the prospect of carbon formation. The latter is noted in the SEM of Fig. 5(b). Over the range of temperatures investigated, H_2:CO ~ 2 as shown in Fig. 10 which indicates that the catalytic conversion process is essentially stoichiometric by Eq. (1).

Fig. 11 shows the results of chemical analysis of the thermal decomposition (bare tube) product gas stream. The H_2:CO ratio now has a comparatively strong dependence on tube wall temperature, and only at high temperature is the ratio stoichiometric (Eq. (1)). The ratio increases to over 3 at 1340 K as temperature is lowered which indicates that additional reactions must be operative. While the species detected by our GC analysis are the same for thermal decomposition and catalytic conversion as shown in the inset to Fig. 11 (which is for 1443 K), it is also likely that additional species will have formed that are not detected by our GC. We did not have the capability to detect additional species with our existing chemical analysis instrumentation.

The reduction of catalytically produced flow rates with the second development of the FIBOR shown in Fig. 8 motivated investigating the influence of prolonged operation on product yields at a given temperature for a specified period of time while monitoring the product flow rate. Fig. 12(a) shows the near constancy of the tube wall temperatures selected for these tests – 990 K and 1190 K-and Fig. 12b shows the corresponding product gas flow rates over a duration of about 4 h at each temperature. At 990 K, the product flow rate is almost constant while at 1190 K a reduction is evident. This reduction is consistent with the sintering decay law of reference [27]. The increase in tube weight shown in Table 1 ("before/after", fifth column) on CT#1 compared to the start of an experiment is the result of the added weight of carbon. For thermal decomposition, the flow rates did not decay to the extent shown in Fig. 12 which is in keeping with the repeatability of product yields shown in Fig. 9. Further work needs to be performed to examine the parameters that control catalyst degradation over time.

3.2.2. Ethylene glycol

Fig. 13 shows the variation of product flow rates for ethylene glycol on CT#2 at two subcoolings. The inset is a representative GC trace at 1233 K. The major species present in the gas stream are CO and H_2, with significant amounts of methane and some C_2H_2 (acetylene) and C_2H_4 (ethylene) also found. Analysis of the GC trace in the inset to Fig. 13 gave the ratio H_2:CO ~ 0.9 at
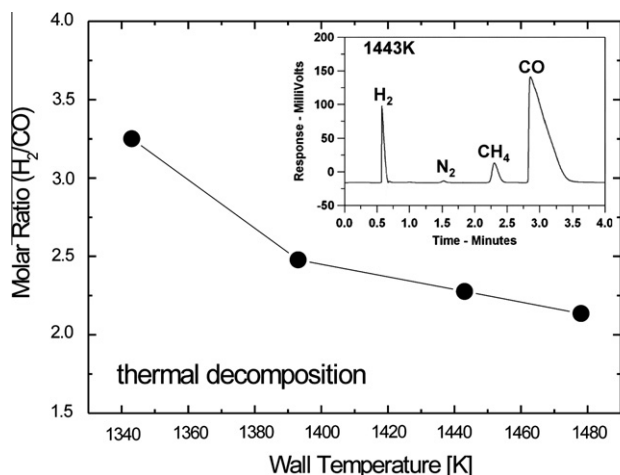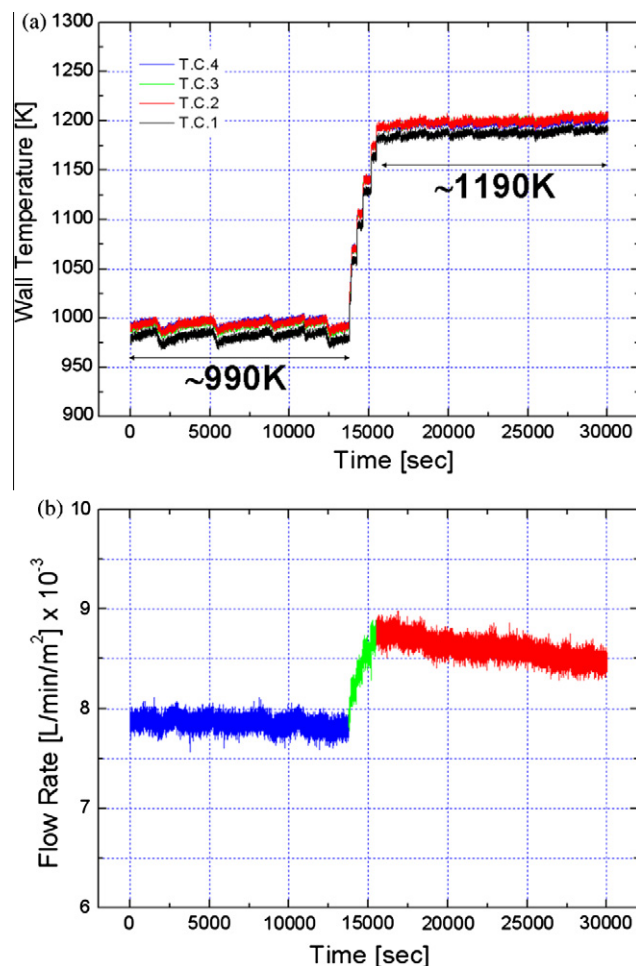
Fig. 12. Endurance test for the CT#1 and methanol showing evolution of tube temperature at two temperatures. Degradation of product flow rate is more evident at the higher temperature during 4 h of operation.

1443 K while the stoichiometric value (from Eq. (2)) is 1.5. These results suggest that the catalytic conversion process of ethylene glycol in the FIBOR may be a multistep process.

The higher subcooling results in Fig. 13 were obtained first, while the lower subcooling data were obtained in a second development of the FIBOR after the liquid level was lowered, power was turned off and the liquid allowed cooling to room temperature. For the first FIBOR, temperature exists for catalytic conversion below which the vapor film cannot be supported (about 1050 K as indicated) and, therefore, the FIBOR no longer exists. At the lower subcooling for the second FIBOR, the vapor film was more stable, film collapse was not observed and there was less scatter in the product flow rate measurements. The shift in the yield shown in Fig. 13 at around 4×10^3 L/min/m^2 and 1150 K to lower temperatures for a subcooling of 42 K is also the result of partial collapse of the vapor film at this temperature which leads to a more efficient overall heat transfer process from the tube and lower average tube temperature.

The lower product flow rates for $\Delta T_{sub} = 25$ K compared to $\Delta T_{sub} = 42$ K in Fig. 13 are counterintuitive, because product yields should increase with decreasing subcooling, as with decreasing subcooling less of the energy input for a given tube temperature would be lost to the bulk and more would go into driving the decomposition reactions. The lower yields at the lower subcoolings may be the result of the catalyst having degraded by undergoing structural changes from the cool-down process, as well as from carbon deposits impeding the reaction process.

Fig. 11. Variation of molar ratio of H_2 to CO with wall temperature for methanol on a bare tube based on GC traces obtained while tube was at the indicated wall temperature (the inset shows a GC trace obtained while T_w was 1443 K). N_2 is from a trickle flow to prevent ignition of methanol vapors.
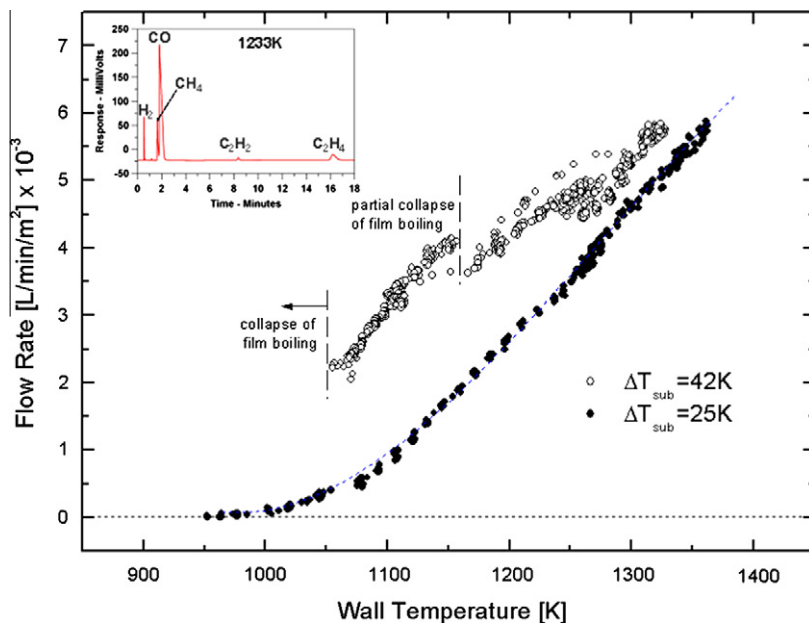
Fig. 13. Variation of product flow rates with T_w for ethylene glycol on CT#2 at the indicated subcoolings. Inset shows product species from a GC trace at 1233 **K**. Solid circle data were obtained after FIBOR was turned off and the ethylene glycol pool allowed to cool to room temperature. Lower temperature limit of FIBOR, determined by destabilization of vapor film, is indicated.

Fig. 14 shows the variation of product flow rate for ethylene glycol on a bare tube with tube surface temperature. The open circle data were obtained on the first FIBOR and the filled circles for the second FIBOR after the liquid level was lowered, power was turned off, the liquid allowed to cool to room temperature and the FIBOR re-formed by the process outlined in Fig. 4. On a bare tube, the surface condition is more consistent and thereby less of a factor in influencing product flow rates for repeated developments of a FIBOR. This leaves thermal considerations associated with a subcooling effect as noted previously.

The inset to Fig. 14 shows a representative GC trace at 1313 K. From this trace the H_2:CO ratio was found to be approximately 0.37, which shows that the thermal decomposition reaction pathway does not proceed entirely by Eq. (2) where H_2:CO = 1.5. Furthermore, as the H_2:CO ratio for CT#2 and a bare tube are not the same (approximately 0.9 and 0.37, respectively), the reaction process for catalytic conversion and thermal decomposition appear to be different. More work is needed to determine these pathways.

The temperature below which product flow rates were undetectable for ethylene glycol (Fig. 14) is lower than the minimum
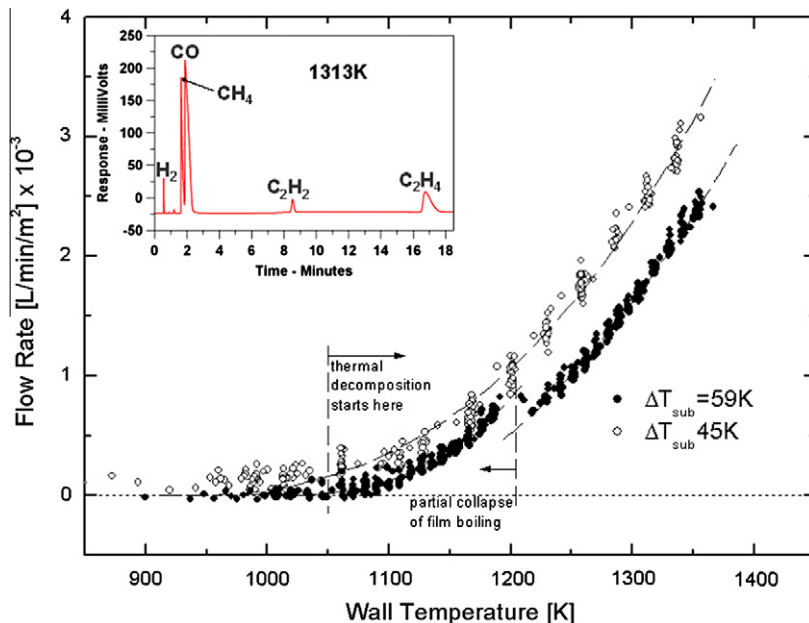
Fig. 14. Variation of product flow rates with T_w for ethylene glycol on a bare tube at two subcoolings. Inset shows product species from a GC trace at 1313 **K**. Solid circle data were obtained after FIBOR was turned off and the ethylene glycol pool allowed to cool to room temperature. Lower temperature limit of FIBOR, determined by destabilization of vapor film, is indicated. There is no reaction below 1050 **K**. For the second FIBOR, partial collapse of film boiling is evident at 1200 **K**.

temperature to maintain the vapor film for catalytic conversion (Fig. 13). As a result, both thermal decomposition and catalytic conversion operate simultaneously for ethylene glycol on CT#2. By contrast, methanol conversion (cf, Figs. 8 and 9) is only by catalytic means over the temperature range covered.

During prolonged operation of the FIBOR, the bulk ethylene glycol temperature was observed to decrease as shown in Fig. 15. The decrease is the result of contamination of the bulk liquid by additional species formed by the decomposition process, as identified by GC/MS analysis of the liquid and by inspection of the ethylene glycol pool which showed discoloration over time. The inset to Fig. 15, and Table 2 shows the species detected by GC/MS analysis. Almost 10% of the liquid impurities have boiling points higher than ethylene glycol. Yet, the bulk liquid temperature dropped over time which suggests that the ethylene glycol/dissolved product mixture might form an azeotrope.

3.3. Conversion efficiency

It is useful to specify the performance of any reactor in terms of an appropriately defined operational efficiency. For a FIBOR this effort is complicated by the fact that no actual work is produced by the conversion process in a FIBOR so that efficiency cannot be based on more traditional thermodynamic definitions. Rather, we look to what a FIBOR is intended to accomplish to develop a measure of its effectiveness.

The function of the FIBOR is to convert a reactant liquid that flows by evaporation into the vapor film. The products are transported away from the film by bubbles. These flows provide a natural definition of a "conversion efficiency", X, as

$$X \equiv \frac{\text{molar flow rate of reactant converted}}{\text{molar flow rate of reactant supplied}}$$

$$= \frac{\dot{N}_{P,out}/v}{\left(\frac{\dot{Q} - A_o \bar{h}(T_{sat} - T_\infty) - \Delta H_{rxn,out}\left(\dot{N}_{P,out}/v\right)}{\int_{T_{sat}}^{T_{out}} C_{P,R} dT + \Delta H_{fg,R}}\right)}. \tag{6}$$

(the right hand side of Eq. (6) is developed in Appendix A). The numerator is the measured molar product gas flow rate divided by v ($X = 0$ means that no liquid is converted or that T_w is too low) and the denominator is the supplied reactant flow rate by the evaporation process.

Figs. 16 and 17 show the variation of X (from measured product flow rates) with T_w for methanol and ethylene glycol, respectively. The assumptions involved in developing the results of Figs. 16 and 17, namely a unimolecular decomposition reaction and a particular correlation for the heat transfer coefficient from the outer surface of the vapor film to the bulk liquid, influence quantitative values of X but not the overall trends (though it was found that the results were not sensitive to the choice of correlation as the heat loss to the subcooled liquid was rather small compared to the energy for evaporation and to drive the reaction). For ethylene glycol especially, the prediction of X is complicated by the fact that the
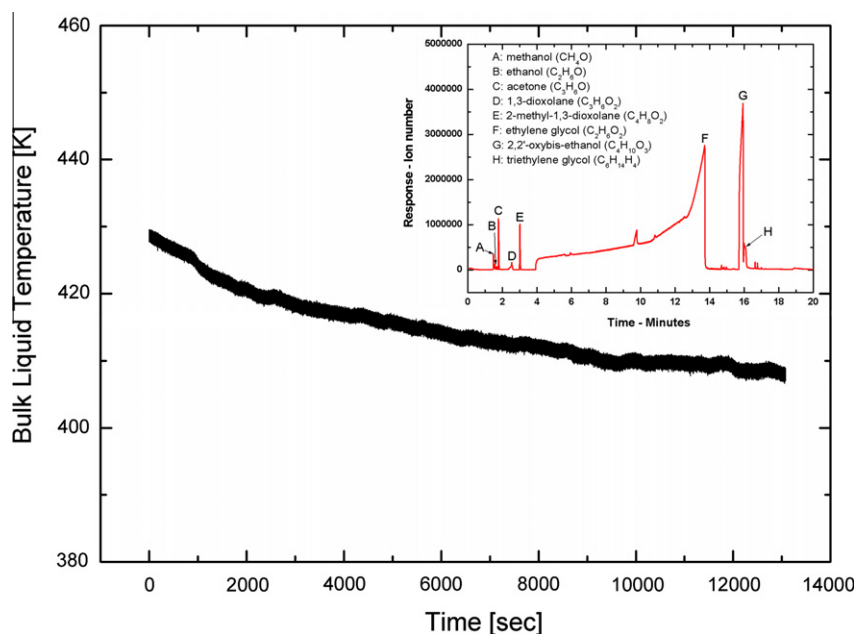
Fig. 15. Evolution of bulk ethylene glycol temperature during operation of a FIBOR on a bare tube. Decrease over time is due to contamination by formation of condensable species. Inset shows a GC/MS analysis of the liquid after FIBOR was turned off and the liquid allowed to cool to room temperature that identifies some of these species.

Table 2
Dissolved species in ethylene glycol.

	Methanol	Ethanol	Acetone	1,3-Dioxolane	2-Methyl-1,3-dioxolane	Ethylene glycol	2,2'-Oxybis-Ethanol	Triethylene glycol
Chemical structure								
Boling point (°C)	65	79	56	75	82	198	246	267
Molecular wt. (g/mol)	32	46	58	74	88	62	106	150
Molar concentration (%)	0.6	0.14	1.6	0.8	1.8	85.3	8.5	1.4
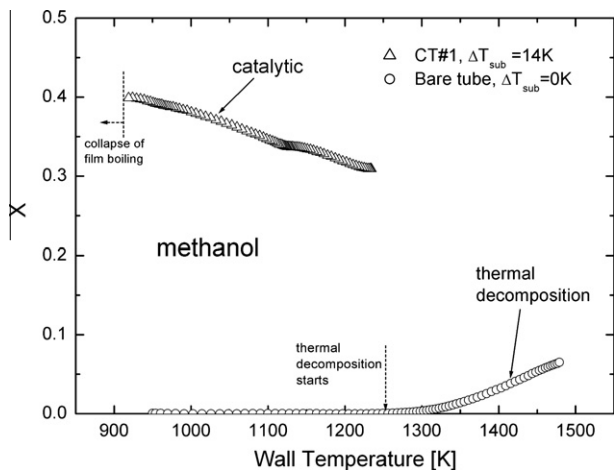
Fig. 16. Methanol conversion on CT#1 (at 14 **K** sub-cooling) and a bare tube (at 0 **K** sub-cooling). Lower limit to catalytic data is determined by film destabilization where FIBOR ceases to exist; lower limit for bare tube is determined by minimum temperature for reactability. FIBOR on CT#1 was not operated above 1250 **K**.
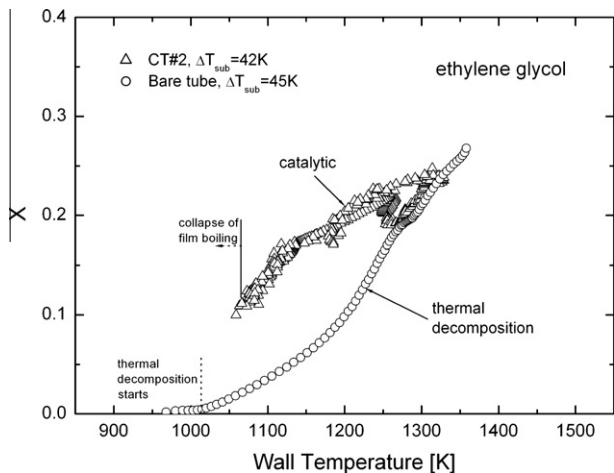
Fig. 17. Ethylene glycol conversion on CT#2 (at 42 **K** sub-cooling) and a bare tube (at 45 **K** sub-cooling). Lower limit to catalytic data is determined by film destabilization where FIBOR ceases to exist; lower limit for bare tube is determined by minimum temperature for reactability. In range where catalytic action would be realized, thermal decomposition also occurs. FIBOR on CT#2 was not operated above 1350 **K**.

conversion is not a unimolecular decomposition process, and that some of the products dissolve into the liquid. These species (i.e., see Table 2) are not considered in the determination of X and for ethylene glycol, X is under predicted. Both catalytic and thermal decomposition conversions are shown in Figs. 16 and 17. The results show that up to 40% methanol and 27% ethylene glycol is converted

For methanol, X decreases with T_w while for ethylene glycol it increases as shown in Figs. 16 and 17. These opposing trends are believed to be a consequence of the ethylene glycol conversion process occurring by both thermal decomposition and catalytic conversion. Over the temperature range investigated, the surface of CT#2 is still hot enough for ethylene glycol to break down by thermal means apart from any catalytic effect. The two conversion routes act in concert with the result being a conversion efficiency that increases with T_w. By contrast, for methanol over the range of temperatures investigated (Fig. 16) the decomposition yields are essentially zero where significant catalytic effects are found.

With only one conversion mechanism for methanol, if the supply rate of methanol (by evaporation) saturates the catalyst then further supplying the film lowers the yield, the overall trend of which is shown in Fig. 16.

4. Conclusions

In this paper, the efficacy of film boiling to promote chemical change of organic liquids has been reported. Product gas flow rates were measured for methanol and ethylene glycol on a horizontal tube and product species were identified. For methanol, the predominant product was synthesis gas suggesting a unimolecular decomposition reaction as the dominant conversion route. For ethylene glycol, additional species were found some of which were condensable and others of which were consistent with the propensity for the tube to be coated with a carbon layer during the film boiling process. The main conclusions are the following:

(1) The reaction process for methanol in film boiling proceeds by unimolecular decomposition to synthesis gas. For ethylene glycol, additional products are found which suggests a more complicated conversion process.
(2) Degradation of the catalyst was observed during prolonged operational times in the FIBOR, as well as when reconstituting a FIBOR after cool-down to room temperature and reheating.
(3) Sub-cooling the reactant liquid made the film boiling process less stable.
(4) Thermal decomposition by film boiling starts at a higher temperature than catalytic conversion. For ethylene glycol, both reaction processes occurred together while for methanol over the temperature range investigated, only conversion occurred only by catalytic means.
(5) For methanol and ethylene glycol which decompose by endothermic reactions, the heat flux needed to maintain the vapor film is higher on a catalyst for a given tube surface temperature, which shifts the film boiling portion of the boiling curves to higher fluxes.
(6) Some of the product species developed for ethylene glycol is soluble in ethylene glycol which was found to lower the bulk liquid temperature over time.
(7) The conversion efficiency in the FIBOR decreased with wall temperature for methanol but increased with temperature for ethylene glycol.

Acknowledgements

Appendix A. Conversion calculation for FIBOR

The conversion of reactant A (where A = methanol or ethylene glycol) for a unimolecular decomposition process $A \to \sum_i \alpha_i B_i$ is defined as

$$X \equiv \frac{\text{molar flow rate of reactant converted}}{\text{molar flow rate of reactant supplied}} = \frac{\dot{N}_{R,in} - \dot{N}_{R,out}}{\dot{N}_{R,in}}$$

$$= \frac{\dot{N}_{P,out}/v}{\dot{N}_{R,in}}, \tag{A1}$$

where

$$\dot{N}_{\mathrm{P,out}} \equiv \sum_i \dot{N}_{B_i,\mathrm{out}}, \tag{A2}$$

and $\sum_i \alpha_i = v$. The assumption of a one-step reaction is an approximation, which is more appropriate for methanol than ethylene glycol. X is a defined quantity and framing the discussion in terms of a one-step reaction does not limit the usefulness of Eq. (A1) as a measure of performance of the FIBOR.

$\dot{N}_{\mathrm{R,in}}$ is the result of evaporation at the boundary of the FIBOR (liquid/vapor interface) and is derived from an energy balance on a control volume that encompasses the vapor film (Fig. 1) as

$$\dot{Q} - \dot{Q}_{\mathrm{sub}} = h_{\mathrm{R,out}}\dot{N}_{\mathrm{R,out}} + h_{\mathrm{P,out}}\dot{N}_{\mathrm{P,out}} - h_{\mathrm{R,in}}\dot{N}_{\mathrm{R,in}}, \tag{A3}$$

where

$$\dot{N}_{\mathrm{R,out}} = \dot{N}_{\mathrm{R,in}} - \dot{N}_{\mathrm{P,out}}/v. \tag{A4}$$

Combining Eqs. (A3) and (A4) gives:

$$\dot{Q} = (h_{\mathrm{R,out}} - h_{\mathrm{R,in}})\dot{N}_{\mathrm{R,in}} + (vh_{\mathrm{P,out}} - h_{\mathrm{R,out}})\left(\dot{N}_{\mathrm{P,out}}/v\right) + \dot{Q}_{\mathrm{sub}}. \tag{A5}$$

Incorporating the specific heat (C_{P}), heat of vaporization (ΔH_{fg}), and heat of reaction (ΔH_{rxn}), and assuming that $T_{\mathrm{in}} = T_{\mathrm{sat}}$, Eq. (A5) becomes:

$$\dot{Q} = \left(\int_{T_{\mathrm{sat}}}^{T_{\mathrm{out}}} C_{\mathrm{P,R}}dT\right)\dot{N}_{\mathrm{R,in}} + \Delta H_{\mathrm{fg,R}}\dot{N}_{\mathrm{R,in}} + \Delta H_{\mathrm{rxn,out}}\left(\dot{N}_{\mathrm{P,out}}/v\right) + A_o \bar{h}(T_{\mathrm{sat}} - T_\infty), \tag{A6}$$

where $T_{\mathrm{out}} = \frac{T_{\mathrm{wall}} + T_{\mathrm{sat}}}{2}$ when the temperature profile in the vapor film is assumed to be linear [17]. The terms on the right hand side of Eq. (A6) are due to the heat input (by resistive heating of the support tube), rate of heat for evaporation of reactant, heat to drive the chemical reaction, and rate of heat loss from the liquid/vapor interface to the bulk liquid by sub-cooling, respectively. Solving for $\dot{N}_{\mathrm{R,in}}$ gives:

$$\dot{N}_{\mathrm{R,in}} = \frac{\dot{Q} - A_o \bar{h}(T_{\mathrm{sat}} - T_\infty) - \Delta H_{\mathrm{rxn,out}}\left(\dot{N}_{\mathrm{P,out}}/v\right)}{\int_{T_{\mathrm{sat}}}^{T_{\mathrm{out}}} C_{\mathrm{P,R}}dT + \Delta H_{\mathrm{fg,R}}}. \tag{A7}$$

Finally, substituting Eq. (A7) into Eq. (A1) gives:

$$X \equiv \frac{\dot{N}_{\mathrm{P,out}}/v}{\left(\frac{\dot{Q} - A_o \bar{h}(T_{\mathrm{sat}} - T_\infty) - \Delta H_{\mathrm{rxn,out}}\left(\dot{N}_{\mathrm{P,out}}/v\right)}{\int_{T_{\mathrm{sat}}}^{T_{\mathrm{out}}} C_{\mathrm{P,R}}dT + \Delta H_{\mathrm{fg,R}}}\right)}, \tag{A8}$$

which is Eq. (6). To compute $\bar{h}$ we used a free convection correlation around a horizontal cylinder [29] with an effective diameter of $d_o + 2\delta$, and assumed that $\delta \ll d_o$ which is an approximation because the liquid/vapor interface thickness is not precisely constant and the interface is in any case not smooth. However, we found that $\dot{Q}$ was substantially greater than the estimated heat loss by subcooling when this correlation for $\bar{h}$ was used.

References

[1] H.M. Higgins, A Study of the Reaction of Metals and Water, AECD-3664, Hanford Atomic Products Operation, Richland, WA, 1955.

[2] W.C. Ruebsamen, F.J. Shon, J.B. Chrisney, Chemical Reaction Between Water and Rapidly Heated Metals, Report NAA-SR-197, North American Aviation, Los Angeles, CA, October, 1952.

[3] R.C. Crooks, P.G. Hershall, H.A. Sorgenti, A.W. Lemmon, R.B. Filbert, Studies Relating to the Reaction Between Zirconium and Water at High Temperatures, Report BMI-1154, Batelle Memorial Institute, Columbus, OH, May, 1962.

[4] B. Lustman, Zirconium–Water Reactions, Report WAPD-137, Bettis Atomic Power Laboratory, Pittsburgh, PA, December, 1955.

[5] M.H. Anderson, P. Meekunnasombat, M.L. Corradini, Experimental behavior of molten SnxLiy when impacted by a vertical column of water, Fusion Technol. 39 (2001) 965–969.

[6] J.P. Herzog, M.L. Corradini, Lithium-lead/water reaction experiments, Fusion Technol. 15 (1989) 979–983.

[7] O. Kranert, H. Kottowski, Studies with respect to the estimation of liquid metal blanket safety, Fusion Eng. Des. 15 (1991) 137–154.

[8] E. Bruneton, B. Narch, B.A. Oberlin, Carbon–carbon composites prepared by a rapid densification process II: structural and textural characterizations, Carbon 35 (1997) 1593.

[9] H. Okuno, H.M. Trinquecoste, A. Derre, M. Monthioux, P. Delhaes, Catalytic effects on carbon/carbon composites fabricated by a film boiling chemical vapor infiltration process, J. Mater. Res. 17 (2002) 1904–1913.

[10] D. Rovillain, M. Trinquecoste, E. Bruneton, A. Derre, P. David, P. Delhaes, Film boiling chemical vapor infiltration: an experimental study on carbon/carbon composite materials, Carbon 39 (2001) 1355–1365.

[11] Y. Zhang, M.N. Gamo, K. Nakagawa, T. Ando, Synthesis of aligned carbon nanotubes in organic liquids, J. Mater. Res. 17 (2002) 2457–2464.

[12] Y.F. Zhang, M.N. Gamo, C.Y. Xiao, T. Ando, Liquid phase synthesis of carbon nanotubes, Physica B 323 (2002) 293–295.

[13] S.A. Zhukov, V.A. Rafeev, S. Yu, S.B. Afans'ev, S.B. Echmaev, B.L. Korsunksii, Singularities of realization of film boiling on wire heaters, High Temp. 41 (2003) 243–251.

[14] K. Okuyama, Y. Iida, Film-boiling heat transfer with a catalytic decomposition reaction, JSME Int. J. B 37 (1994) 123–131.

[15] M. Epstein, J.C. Leung, G.M. Hauser, R.E. Henry, Film boiling on a reactive surface, Int. J. Heat Mass Transfer 27 (1984) 1365–1378.

[16] Y.Q. Zhou, J.W. Rose, Effect of 2-dimensional conduction in the condensate film on laminar-film condensation on a horizontal tube with variable wall temperature, Int. J. Heat Mass Transfer 39 (1996) 3187–3191.

[17] B.J. Urban, C.T. Avedisian, W. Tsang, The film boiling reactor: a new environment for chemical processing, AIChE J. 52 (2006) 2582–2595.

[18] C.T. Avedisian, W. Tsang, T. Davidovits, T.J.R. Allaben, Influence of radiation on product yields in a film boiling reactor, AIChE J. 54 (2008) 575–581.

[19] C.L. Yaws, Handbook of Thermodynamic and Physical Properties of Chemical Compounds, Knovel, 2003. Online Database Available at: <http://knovel.com>.

[20] J.W. Shabaker, G.W. Huber, R.R. Davda, R.D. Cortright, J.A. Dumesic, Aqueous-phase reforming of ethylene glycol over supported platinum catalysts, Catal. Lett. 88 (2003) 1–8.

[21] H. Xun, L. Gongxuan, Investigation of the steam reforming of a series of model compounds derived from bio-oil for hydrogen production, Appl. Catal. B 88 (2009) 376–385.

[22] J.W. Evangelista, An experimental demonstration of converting organic liquids and their aqueous solutions in a film boiling reactor, M.S. Thesis, Cornell University, 2010.

[23] S.R. Choi, On film boiling to promote chemical change of organic liquids, PhD Thesis, Cornell University, 2010.

[24] A.J. Ede, J.B. Siviour, Sub-cooled film boiling on horizontal cylinders, Int. J. Heat Mass Transfer 18 (1975) 737–742.

[25] Y. Fugita, Q. Bai, Critical heat flux of binary mixtures in pool boiling and its correlation in terms of Marangoni number, Int. J. Refrig. 20 (1997) 616–622.

[26] K.H. Sun, J.H. Lienhard, The peak pool boiling heat flux on horizontal cylinders, Int. J. Heat Mass Transfer 13 (1970) 1425–1439.

[27] H.S. Fogler, Elements of Chemical Reaction Engineering, 4th ed., Pearson Publishing, Westford Massachusetts, 2006. pp. 709–716.

[28] T. Baird, Z. Paal, S.J. Thomson, Sintering studies on platinum black catalysts, J. Chem. Soc. Faraday Trans. 1 (69) (1973) 50–55.

[29] S.W. Churchill, H.H.S. Chu, Correlating equations for laminar and turbulent free convection from a horizontal cylinder, Int. J. Heat Mass Transfer 18 (1975) 1049.